

## ON SOME PARAMETERS OF THE FERMI SURFACE IN MOLYBDENUM

V. V. BOIKO and V. A. GASPAROV

Submitted June 14, 1971

Zh. Eksp. Teor. Fiz. 61, 1976-1985 (November, 1971)

The radio-frequency size effect in molybdenum samples cut out along the (100) and (110) planes is investigated. The anisotropy of the extreme dimensions of small parts of the Fermi surface of the metal is determined and the shapes of electron surface of the lens and spheroids types and of hole ellipsoids are reconstructed. Carriers with an extreme displacement over a period are observed. The values of  $|\partial S/\partial k_H|_{\text{extr}}$  are measured and the cross sections of the electron jack and hole octahedron to which the carriers belong are found.

## INTRODUCTION

THE investigation of the Fermi surface of molybdenum, a model for which was proposed in <sup>[1,2]</sup>, has by now been the subject of many experimental papers. Such investigations were undertaken by practically all known experimental-physics methods for studying the electron structure of metals. The most detailed information, however, was obtained from measurements of the de Haas-van Alphen effect,<sup>[3,4]</sup> cyclotron resonance,<sup>[5]</sup> and the radio-frequency size effect.<sup>[6]</sup> As a result of these experiments it was established that the Fermi surface of molybdenum is closed and consists of a complicated electron surface and several hole surfaces. The area and dimensions of the extremal sections of the hole ellipsoids and of the electron-jack octahedron were determined. The effective masses of the individual conduction-electron groups were determined and their anisotropy in the planes (110) and (121) was investigated.

Although considerable experimental information has already been accumulated concerning the energy spectrum of this metal, nonetheless individual sections of its Fermi surface have not yet been reconstructed. This pertains mainly to the most complicated part—the electron jack, and more accurately to the spheroids located at its ends. The experimental results for them are not only incomplete but also contradictory, because the dimensions of these spheroids are close to the dimensions of the hole ellipsoids and consequently difficulties arise in the interpretation of the experimentally observed curves.

Since the exact form of the Fermi surface of molybdenum is very important for further theoretical calculations of the energy spectra of transition metals, it is of interest to carry out additional investigations in order to obtain reliable experimental information not only for the indicated sections of this surface, but also for the sections with the extremal value of  $|\partial S/\partial k_H|$ , for which there is at present no information whatever. The present communication is devoted to the results of these investigations.

## EXPERIMENT

To solve our problem, we chose the method of the radio-frequency size effect.<sup>[7]</sup> In experiments performed at 3.5 MHz and 1.5–4.2°K, using a modulation

procedure, we measured the active part of the surface impedance  $Z = R + iX$  of thin ( $l \sim d$ ) plane-parallel molybdenum plates as functions of the magnetic field ( $l$ —mean free path of the conduction electrons,  $d$ —sample thickness). These dependences revealed a number of singularities, the positions of which in a magnetic field parallel to the surface of the sample are connected with the dimension  $2k$  of the extremal orbit in the  $n \times H$  direction and with the thickness  $d$  of the sample by the following relation:

$$2k = eHd / ch; \quad (1)$$

here  $n$  is the normal to the sample surface,  $e$  the electron charge,  $c$  the speed of light,  $k$  the wave vector, and  $h$  Planck's constant.

By investigating the positions of these singularities in terms of the field as a function of the angle of rotation of the magnetic field  $H$  relative to the crystallographic directions of the sample, we obtained the extremal dimensions of the electron orbits along different directions in the crystal.

The experimental setup used for the measurements was described in detail in <sup>[6]</sup>. In the present experiments it was improved to be able to register both the first derivative  $\partial R/\partial H$  and the second derivative  $\partial^2 R/\partial H^2$  of the active part of the surface impedance of molybdenum with respect to the field, and to perform measurements in a wide range of angles of inclination of the magnetic field relative to the sample surface.

When plotting the second derivative, the synchronous detection was effected at double the magnetic-field modulation frequency  $2\Omega$  ( $\Omega = 18$  Hz).

The modified low-temperature part of the setup is shown in Fig. 1. The sample 1, placed vertically in a two-section coil 2, was glued with the aid of two pieces of cigarette paper 3 to a quartz flat-head pin 4, the post of which passed through an opening in quartz plate 5 and was clamped by grip 6. A worm gear 7–8 rotated the sample in the vertical plane. The coaxial cable 9 and the clamping contacts 10 were used to connect the coil 2, which was glued to the quartz plate 5, to the remainder of the generator circuit, which was kept at room temperature. The entire assembly was placed inside a cylindrical copper vessel 11, sealed by a ground joint 12 and filled with helium gas.

Such a system for placing and rotating the object had a number of significant advantages.

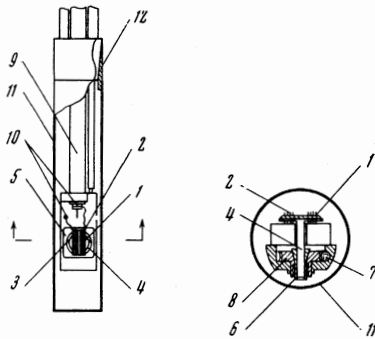


FIG. 1. Low-temperature part of the generator and the system for rotating the sample (the callouts are given in the text). The scale for the section shown on the right is increased by a factor of 2.

First, it made it possible to perform experiments under the most convenient conditions, since the investigated sample was rotated independently of the induction coil, and consequently the requirement that the high-frequency electric and constant magnetic fields remain mutually perpendicular or parallel (if the coil was fastened horizontally) was fulfilled for all crystallographic directions of the crystal.

Second, in combination with the system for rotating the magnet, which was rotated in a horizontal plane, it made it possible to orient the magnetic field relative to these directions with a high degree of accuracy and to perform measurements in either a parallel magnetic field or in a field making an arbitrary angle with the sample surface.

The field orientation relative to the crystallographic directions was established on the basis of the symmetry of the experimental curves, and parallelism between the field and the sample surface was established by setting the signal in the strong field at a minimum.

The molybdenum samples were disks of nearly circular or elliptic shape. They were cut by the electric-spark method from single-crystal ingots with  $R(300^\circ\text{K})/R(4.2^\circ\text{K}) \approx 1.8 \times 10^4$ . To improve the quality of their surfaces and to decrease the thickness scatter, they were ground with M-10 silicon-carbide powder.

To remove the surface layer damaged as a result of such a processing, the ground disks were etched in a composition described by us earlier.<sup>[6]</sup> The etching rate was varied by adding water to this etchant. Investigations have shown that it suffices to etch off 0.05 mm

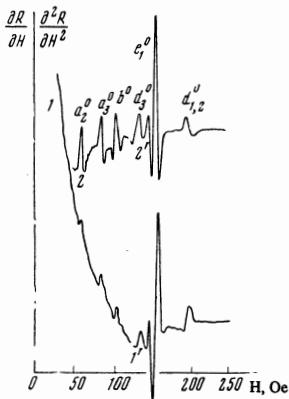


FIG. 2. Typical plot of size-effect lines for a sample with  $n \parallel [100]$ ,  $d = 0.263$  mm,  $T = 4.2^\circ\text{K}$ ,  $f = 3.8$  MHz,  $H \parallel [001]$ ,  $E \perp H$ . Curves 1—plot of  $\partial R/\partial H$ , curve 2—plot of  $\partial^2 R/\partial H^2$ . The gain used to plot curves 1' and 2' was decreased by a factor of 10.

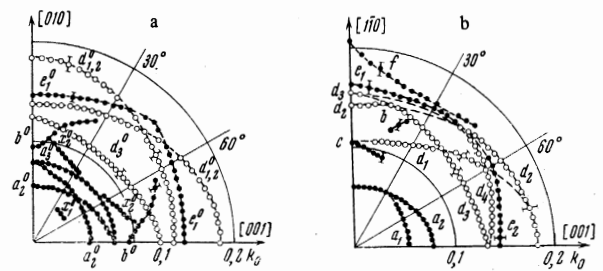


FIG. 3. Angular dependence of the half-width of small extremal orbits (in units of  $k_0$ ): a—in the (100) plane, b—in the (110) plane. The dark and light circles mark lines belonging to the electron and hole surfaces, respectively.

from these disks to eliminate the damaged layer completely. This was extremely important when samples oriented in the (100) plane were prepared, since deeper etching produced deep ruts on their surfaces, which caused considerable broadening of the size-effect lines.

The sample orientation was monitored by x-ray diffraction with accuracy  $\pm 30'$ , and the thickness was measured with a vertical optical caliper ( $\pm 1 \mu$ ).

## MEASUREMENT RESULTS

The measurements were performed on molybdenum samples with normals to the surface  $n \parallel [100]$  and  $n \parallel [110]$ . A typical plot of the size-effect lines observed in weak fields in the (100) plane is shown in Fig. 2.

As seen from the figure, owing to registration of the second derivative of the active surface-impedance part of the samples with respect to the field, it was possible to eliminate the strong nonmonotonic field dependence observed in the plot of  $\partial R/\partial H$ , and to register the size-effect lines against the background of an almost horizontal null line, separating them more distinctly from one another. This has made it possible not only to increase the accuracy with which the positions of these lines relative to the field were measured, but also to observe a number of new lines which could not be resolved earlier.<sup>[6]</sup>

The determined extremal dimensions of the small sections of the molybdenum Fermi surface in the (100) and (110) planes are represented by the polar diagrams of Fig. 3. The wave vector  $k$ , determined from formula (1), was measured in a radial direction in units of  $k_0$  ( $k_0 = 1.998 \text{ \AA}^{-1}$  is the limiting wave vector of the Brillouin zone of molybdenum in the [100] direction). The value of  $H_0$ , which was needed for the calculation, was determined from the left ends of the lines. The reference point was selected on the basis of the results of an investigation of the frequency dependence of the positions of the extrema of the size-effect lines in metals<sup>[8, 9]</sup> as well as the results in comparing the same Fermi-surface parameters obtained with the aid of the radio-frequency size effect and other investigation methods.<sup>[10, 11]</sup> All the values of  $k$  were determined at  $H$  parallel to the sample surface and with the electric and magnetic fields polarized such that  $E \perp H$ . The maximum error in the determination of the indicated quantity does not exceed  $\pm 4\%$ .

A study of the behavior of the observed lines when the magnetic field is inclined to the sample surface has made it possible to establish that three of them,  $b$ ,  $b^0$ , and  $f$ , split when the magnetic field is inclined, whereas all others shift towards stronger fields without splitting, gradually decreasing in intensity. Investigations in an inclined field have also made it possible to observe a number of additional lines, which are seen only in samples cut in the (110) plane. Typical lines are shown in Fig. 4. Such lines appear when the magnetic field is inclined in the  $([1\bar{1}0], n)$  plane, starting with an angle of  $14^\circ$  between  $H$  and  $[1\bar{1}0]$ . With increasing field inclination, this line, shifting towards stronger magnetic fields, gradually increases in intensity, reaching a maximum intensity when the angle between  $H$  and  $[1\bar{1}0]$  is  $45^\circ$ . Further increase of the inclination of the magnetic field broadened the lines and decreased the amplitudes. At an angle of  $79^\circ$  the lines vanished and gave way to harmonic oscillations which existed at angles  $80-90^\circ$  between  $[1\bar{1}0]$  and  $H$  (Fig. 5).

Such lines were observed at high-frequency current polarizations  $j \parallel [001]$  as well as  $j \parallel [1\bar{1}0]$ . They turned out to be strictly periodic in the field. The dependence of their period on the inclination of the magnetic field is shown in Fig. 6.

## DISCUSSION OF RESULTS

As already noted in <sup>[6]</sup>, the Fermi surface of molybdenum consists of six hole ellipsoids, an octahedron, and an electron jack and lenses. We start the discussion of the results obtained in the present communication (Fig. 3) with the simplest part of the surface, the hole ellipsoids. There can be no doubt that the lines  $d$  correspond to these ellipsoids. Two of these lines,  $d_3$  and  $d_4$  (Fig. 3b) describe well the shadow projections of the ellipsoids on the (110) plane, and all others ( $d_{1,2}$ ,  $d_3^0$ ,  $d_4^0$ ,  $d_1$ ,  $d_2$ ) give directly their central sections by the planes (100) and (110). Such sections confirm the theoretical that the hole ellipsoids are not figures of revolution. Their long axis  $a = 0.37 \text{ \AA}^{-1}$  is directed along  $[001]$ , and the others,  $b = 0.29 \text{ \AA}^{-1}$  and  $c = 0.22 \text{ \AA}^{-1}$ , are directed along  $[110]$  and  $[1\bar{1}0]$ .

It is also possible to determine uniquely the shape, dimensions, and orientation of the electron lenses relative to the principal crystallographic directions. The

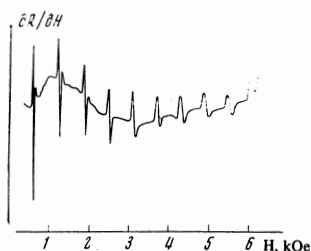


FIG. 4

FIG. 4. Typical size-effect lines in an inclined field for a sample with  $n \parallel [110]$ . The magnetic field is inclined in the  $([1\bar{1}0], n)$  plane and the angle between  $[1\bar{1}0]$  and  $H$  is  $45^\circ$ ;  $f = 3.5 \text{ MHz}$ ,  $T = 4.2^\circ \text{ K}$ ,  $d = 0.245 \text{ mm}$ .

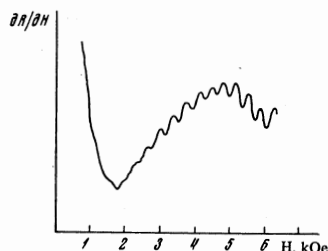


FIG. 5

FIG. 5. Typical plot of size effect in a magnetic field normal to the sample surface:  $n \parallel [110]$ ,  $f = 3.5 \text{ MHz}$ ,  $T = 4.2^\circ \text{ K}$ ,  $d = 0.239 \text{ mm}$ .

anisotropy of lines  $a$  indicates that these lenses have the shape of a cone whose base and apex are rounded.<sup>[6]</sup> These lines are round in the intersection with the plane (100), which is described by the line  $a_3^0$ , and elongated in the  $[001]$  direction (line  $a_2$ ); this is in full agreement with the data obtained earlier in <sup>[6]</sup>.

As to all the remaining lines ( $b^0$ ,  $e_1^0$ ,  $x_1^0$ ,  $x_2^0$ ) (Fig. 3a) and  $b$ ,  $e_1$ ,  $e_2$ ,  $c$ ,  $f$  (Fig. 3b) it would be natural to identify them with the electron jack.

The angle interval in which the lines  $b$  and  $b^0$  exist and their anisotropy make it possible to attribute them to orbits passing through the necks joining the central part (octahedron) of the electron surface with the spheroids. Although at some orientations of the magnetic field these lines split when the field is inclined relative to the sample surface, nonetheless this does not contradict our interpretation inasmuch as is evidenced by the analysis, a contribution to their amplitude is made also by the electrons of the noncentral sections, which are the ones responsible for the observed splitting. From the dimensions determined from these lines it follows that in the intersection with the (100) plane the neck has a shape close to a circle with a diameter  $0.36 \text{ \AA}^{-1}$ .

The lines  $e_1^0$ ,  $e_1$ , and  $e_2$  could be attributed only to orbits passing through the spheroids. Since information concerning the shape and dimensions of these parts of the electron surface is presently quite contradictory, owing to the considerable difficulties entailed in the interpretation of the experimental data, we shall stop to discuss in greater detail the interpretation of our results.

The anisotropy of the lines  $e_1^0$ ,  $e_1$ , and  $e_2$  is evidence that the central section of these spheroids in the (100) plane is not round, as assumed in all the preceding experimental papers, but is a square with rounded corners. Favoring this assumption is also the behavior of the intensities of the lines  $e$ . When the magnetic field is oriented along  $[001]$  in the (100) plane and along  $[1\bar{1}0]$  in the (110) plane, the amplitude of these lines increases sharply, a fact that can be attributed only to the increase of the time of interaction of the electrons with the electromagnetic wave since the flat sections of their trajectories enter in the skin layer, and to the broadening of the strip of sections that contribute to the size effect. On the basis of the lines  $e_1^0$ ,  $e_1$ , and  $e_2$ , we succeeded in reconstructing completely the central section of the spheroids in the (100) plane and in determining its main dimensions (Fig. 7).

The validity of the foregoing results can also be verified easily by using the dimensions determined by the lines  $x_1^0$ ,  $x_2^0$ , and  $c$ , the origin of which is due to

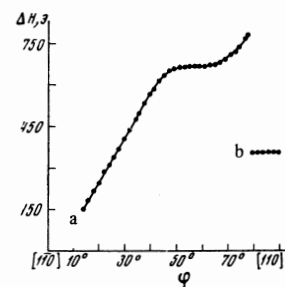


FIG. 6. Angular dependence of the period  $\Delta H$  of the size-effect lines: a—lines shown in Fig. 4, b—lines corresponding to Fig. 5.

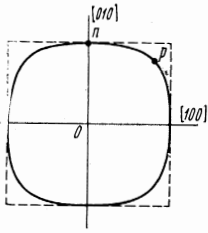


FIG. 7

FIG. 7. Central section of spheroid in the (100) plane, reconstructed from the experimental data.  $O_n = 0.29 \text{ \AA}^{-1}$ ,  $O_p = 0.33 \text{ \AA}^{-1}$ .

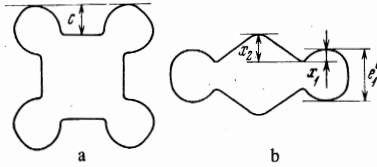


FIG. 8

FIG. 8. Measured dimensions of central section of electron jack, a—(110) plane,  $H \parallel [001]$ ; b—(100) plane,  $H \parallel [011]$ .

the presence of several effective points on the electron trajectories represented in Fig. 8.

Unfortunately, it is impossible to compare quantitatively all these data with the presently available theoretical calculations,<sup>[1, 2]</sup> since the corresponding information is not given in the cited papers. We can nevertheless note that the shape established by us for the sections of this surface agrees well with the Loucks theory.<sup>[2]</sup>

Of all the lines shown in Fig. 3, the only one determined completely by noncentral sections of the electron surface was f. This was evidenced by its behavior with changing inclination of the magnetic field relative to the sample surface. Starting with field inclination angles of  $0.5^\circ$ , the line split into two lines that diverged in opposite directions. Although we were unable to relate it uniquely to a definite section of the indicated surface, nonetheless we propose that it is due to orbits passing through the body and the necks of the four spheres of the electron jack, a hypothesis favored not only by the anisotropy of the line but also by its measured dimension.

We now proceed to an interpretation of those lines where were observed by us at large inclinations of the magnetic field (Figs. 4 and 5). The angular dependence of the period (Fig. 6) and the character of the behavior of these lines with changing field inclination indicate that they are due to two different carrier groups belonging to sections of the Fermi surface with extremal value of  $|\partial S/\partial k_H|$ .

Such carriers, as is well known,<sup>[12]</sup> produce in the interior of the metal, at distances determined by the formula

$$U = \frac{c\hbar \sin \varphi}{eH} \left| \frac{\partial S}{\partial k_H} \right|_{\text{ext}} \quad (2)$$

electromagnetic-field spikes whose emergence from the opposite side of a plane-parallel plate leads to the size-effect lines. Here  $\varphi$  is the angle of inclination of the magnetic field to the sample surface, S the area of intersection of the Fermi surface with the plane  $k_H = \text{const}$ , and  $k_H$  is the projection of the wave vector in the magnetic-field direction.

The first carrier group, causing the lines shown in Fig. 4, can be related, owing to the large angle interval in which they exist, to the shape, and to the considerable intensity of these lines, with the "effective" sections of the hole octahedron. The possibility of the existence of

such sections on the indicated part of the Fermi surface of molybdenum can easily be verified by plotting  $|\partial S/\partial k_H|$  against  $k_H$  for a regular octahedron. If the magnetic field is inclined in the plane of the figure, as shown in Fig. 9, then the area of the octahedron section will be connected with the angle of inclination  $\varphi$  of the magnetic field ( $0^\circ \leq \varphi \leq 45^\circ$ ) and the projection  $k_H$  of the wave vector on the field direction by the following relations:

$$S = \frac{\sqrt{2}(k^0)^2}{\cos \varphi} - \frac{2\sqrt{2}k_H^2}{\cos 2\varphi \cdot \cos \varphi},$$

when  $k_H$  varies from 0 to  $K \equiv k^0 (\cos \varphi - \sin \varphi)/\sqrt{2}$ , and

$$S' = \frac{1 + \text{tg} \varphi}{\sqrt{2} \sin \varphi} \left[ k^0 - \frac{\sqrt{2}k_H}{\cos \varphi + \sin \varphi} \right]^2$$

for  $k_H$  ranging from K to  $k^0$  ( $k^0$  is half the diagonal of the square).

The derivatives of these expressions with respect to  $k_H$  reach a maximum at  $k_H = K$  and exhibit a kink. The value of  $(\partial S/\partial k_H)_{\text{max}}$  at these points varies with changing magnetic field inclination in accordance with the law

$$\left( \frac{\partial S}{\partial k_H} \right)_{\text{max}} = - \frac{4k^0}{(\cos \varphi + \sin \varphi) \cos \varphi}. \quad (3)$$

A similar expression can also be written for the condition  $45^\circ \leq \varphi \leq 90^\circ$ , but in this case the denominator will be  $\sin \varphi$  rather than  $\cos \varphi$  multiplied by the sum  $\cos \varphi + \sin \varphi$ .

The section of an octahedron having such an extremum, clinging as it were to its vertex  $A_1$  (Section  $A_1B_1$  in Fig. 9), shifts gradually towards the central section with increasing inclination of the magnetic field. At  $\varphi = 45^\circ$  it passes in the immediate vicinity of the central section, and then, clinging to the second vertex  $A_2$  (Section  $A_2B_2$ ), it moves away from it.

The carriers belonging to these sections are "effective" in large intervals of inclination angles of the magnetic field, since the "effectiveness" strip of the octahedron fully encloses its side faces. Therefore the plate surface-impedance singularities due to such carriers should have the form of sharp peaks, as is indeed observed in the experiments.

A plot of (3) is shown in Fig. 10. We used in the calculations the value  $k^0 = 0.88 \text{ \AA}^{-1}$ , determined from the data of [6]. The same figure shows the results of the

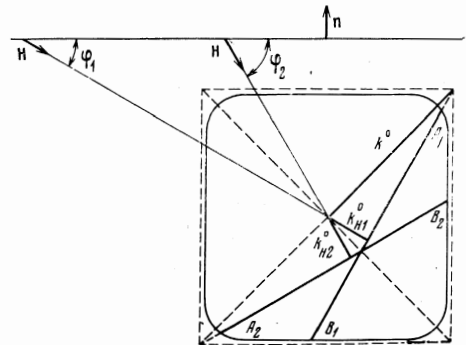


FIG. 9. Section of hole octahedron in the plane (100), illustrating the positions of the orbits with extremal value of  $|\partial S/\partial k_H|$ .

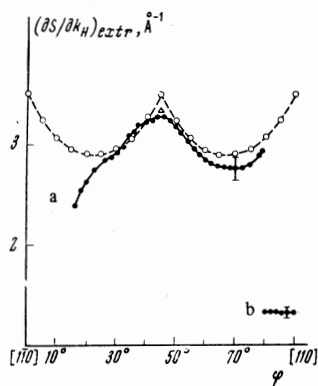


FIG. 10. Angular dependence of  $|\partial S/\partial k_H|_{\text{extr}}$  of the carriers responsible for the sharp peaks (a) and harmonic oscillations (b) in the surface impedance of molybdenum:  $\circ$ —calculation by formula (3),  $\Delta$ —value obtained by graphic differentiation of the plot of  $S(k_H)$  of the real model at an angle of  $45^\circ$  between  $[110]$  and  $H$ ,  $\bullet$ —results of experiment.

present experiment (curve a), reduced in accordance with the formula

$$\left| \frac{\partial S}{\partial k_H} \right|_{\text{extr}} = \frac{ed}{\hbar c} \frac{\Delta H}{\sin \varphi}, \quad (4)$$

which can easily be obtained from (2).

The discrepancies near  $45^\circ$  and  $70^\circ$  are undoubtedly due to the rounding of the corners and edges of the hole octahedron of molybdenum. As a result, the plot a has a smooth rather than a jumplike character. The deviation in the region of small inclinations of the magnetic field, on the other hand, is possibly connected with the fact that in this angle interval the observed size-effect lines are not due to the holes but to the electrons of the central sections of the electron surface, which have at these magnetic-field inclination angles a displacement into the interior of the metal, per period, close to that of the holes. With increasing field inclination angle, the contribution of these sections decreases, and at angles  $\varphi > 30^\circ$  the size-effect lines are determined mainly only by the section of the hole octahedron. Although such an explanation is not unambiguous, the presence of an inflection in the function  $|\partial S/\partial k_H|_{\text{extr}}$  at  $\varphi \approx 32^\circ$  is evidence in its favor.

The carriers belonging to the electron surface are obviously responsible also for the harmonic oscillations of the surface impedance of molybdenum, which were observed by us in a magnetic field normal to the sample surface (Fig. 5). At this magnetic-field orientation, according to the theoretical calculation,<sup>[2]</sup> there should exist on the electron jack three orbits that are extremal with respect to the area: the orbit on the spheroids, the orbit passing over two spheroids and the edge of the

electron octahedron, and the orbit passing over the central part of the electron surface. Naturally, sections with extremal values of  $|\partial S/\partial k_H|_{\text{extr}}$  exist between the last two types of orbits. As shown by qualitative analysis, such sections pass over the electron octahedron near its necks. The electrons belonging to these sections are not effective, and  $|\partial S/\partial k_H|_{\text{extr}}$  varies little with inclination of the magnetic field, at least in an interval of  $10^\circ$ , in agreement with the experimental data (Fig. 10) obtained from the dependence of the period of the harmonic oscillations of the surface impedance of molybdenum (Fig. 6).

Thus, our investigations have enabled us to reconstruct fully the shape and dimensions of the small sections of the Fermi surface of molybdenum, to observe carriers with extremal displacement per period, to determine the values of  $|\partial S/\partial k_H|_{\text{extr}}$  and to show that the sections to which such carriers belong exist not only on the electron jack but also on the hole octahedron.

In conclusion, it is our pleasant duty to thank G. N. Landysheva for help with the experiments.

<sup>1</sup>W. M. Lomer, Proc. Phys. Soc. **84**, 327 (1964).

<sup>2</sup>T. L. Loucks, Phys. Rev. **139**, A1181 (1965).

<sup>3</sup>D. M. Sparlin and J. A. Marcus, Phys. Rev. **144**, 484 (1966).

<sup>4</sup>G. Laaver and A. Myers, Phil. Mag. **19**, 465 (1969).

<sup>5</sup>R. Herrmann, Phys. Stat. Sol. **25**, 427 (1968).

<sup>6</sup>V. V. Boiko, V. A. Gasparov and I. G. Gverdsiteli, Zh. Eksp. Teor. Fiz. **56**, 489 (1969) [Sov. Phys.-JETP **29**, 267 (1969)].

<sup>7</sup>V. F. Gantmakher, ibid. **44**, 811 (1963) [17, 549 (1963)].

<sup>8</sup>I. P. Krylov and V. F. Gantmakher, ibid. **51**, 740 (1966) [24, 492 (1967)].

<sup>9</sup>A. Fukumoto and H. W. P. Strandberg, Phys. Lett. **23**, 200 (1966).

<sup>10</sup>J. E. Koch and T. K. Wagner, Phys. Rev. **151**, 467 (1966).

<sup>11</sup>V. F. Gantmakher, Progr. in Low Temp. Phys. **5**, 181 (1967).

<sup>12</sup>V. F. Gantmakher and É. A. Kaner, Zh. Eksp. Teor. Fiz. **48**, 1572 (1965) [Sov. Phys.-JETP **21**, 1053 (1965)].